

# 利用 CFD 技术对城市生活垃圾富氧燃烧特性分析

刘国辉, 马晓茜, 余昭胜

(华南理工大学 电力学院, 广东 广州 510640)

**摘 要:** 富氧燃烧技术具有明显的节能与环保效益, 是低热值垃圾稳燃, 减少污染物排放的有效措施。运用 CFD 技术对垃圾在机械炉排炉内富氧气氛下的燃烧特性进行了研究, 给出了  $O_2/N_2=21:79$  和  $O_2/N_2=25:75$  两种工况下床层上方的烟气温、烟气组分浓度曲线及床层焦炭分布图。模拟结果表明: 当一次风的氧气浓度由 21%(v) 提高到 25%(v) 时, 垃圾床层表面燃烧区域平均温度由 1 350 K 升高到了 1 466 K, 增加了 116 K; 灰渣中可燃物(焦炭)含量由 3.9%(wt) 降为 0.1%(wt), 随着氧气浓度增加, 垃圾着火位置前移, 提前进入稳定燃烧阶段。模拟结果与前人的试验测量值吻合。

**关 键 词:** 生活垃圾; 焚烧; 富氧; 数值模拟; 马丁往复炉排

中图分类号: TK224.1 文献标识码: A

符号说明

- $\rho_{sh}$ —床层的大体积密度/ $kg \cdot m^{-3}$ ;
- $V_B$ —炉排的运动速度/ $m \cdot s^{-1}$ ;
- $H_s$ —固体颗粒的焓/ $J \cdot kg^{-1}$ ;
- $S_s$ —垃圾水分蒸发、热解、焦炭燃烧速率/ $g \cdot m^{-3}$ ;
- $Q_{sh}$ —垃圾固相热源/ $W \cdot m^{-3}$ ;
- $\tau$ —料层内的剪切力张量;
- $T_s$ —垃圾料层温度/K;
- $Y_{is}$ —颗粒中各组分(水分、挥发分、焦炭、灰分)的质量分数;
- $D_s$ —固体颗粒的混合系数/ $m^2 \cdot s^{-1}$ ;
- $V_s$ —垃圾颗粒的平均运动速度/ $m \cdot s^{-1}$ ;
- $g$ —重力加速度/ $N \cdot kg^{-1}$ ;
- $\sigma$ —料层内的法线压力张量;
- $\lambda_s$ —垃圾料层的导热率/ $W \cdot (m \cdot K)^{-1}$

## 引 言

焚烧处理技术能使被处理的垃圾减容、减重, 并达到无害化、资源化, 但其燃烧过程却会产生大量的有害物质, 引发严重的环境问题。为了使燃烧更加完全, 同时减少有毒有害物质的生成, 必须控制好垃圾燃烧温度、氧气浓度及烟气停留时间。然而, 由于我国生活垃圾的热值低、水分高, 导致焚烧炉的温度往往偏低, 常常需要投油助燃才能保证炉膛温度。富氧燃烧不仅能提高垃圾燃烧温度, 促进有害有机

物的分解, 还能减少  $CO$ 、 $NO_x$ 、 $PCDDs$  等污染物的排放, 是一种能够综合控制垃圾焚烧的新型洁净燃烧技术<sup>[1~5]</sup>。

由于垃圾焚烧炉结构复杂, 影响因素较多, 原型及模型的冷热实验所消耗的人力物力较大; 且受测试条件及所用仪器的影响, 很难获得满意的结果。虽然现有的数学模型不够准确或精确, 但数值模拟能对焚烧炉内的速度场、浓度场、温度场做全面的分析和对比, 已成为了有力的研究工具。鉴于国内还未将富氧燃烧技术运用于生活垃圾焚烧发电厂, 为了能和实际情况作对比, 选取了德国 Coburg 垃圾发电厂的 2 号焚烧炉为研究对象, 运用流体动力学专业计算软件 Fluent 和英国设菲尔德 (Sheffield) 大学废弃物处理中心提出的床层模型<sup>[6~8]</sup>, 对焚烧炉在额定处理量下进行了富氧燃烧数值模拟研究, 并将数值计算结果与前人的试验数据进行对比分析。

## 1 德国 Coburg 生活垃圾焚烧发电厂<sup>[2]</sup>

### 1.1 焚烧炉概况

德国 Coburg 生活垃圾发电厂, 配有两台焚烧炉, 单台处理量为 7 t/h。一体化余热锅炉, 炉型为逆流式, 炉排为马丁往复机械炉排。一次风从炉排下方的风室进入燃烧炉膛, 共分五级配置; 前后墙各有两排二次风口。经合理简化后的焚烧炉结构如图 1 所示。入炉生活垃圾的元素分析和工业分析如表 1 所示。

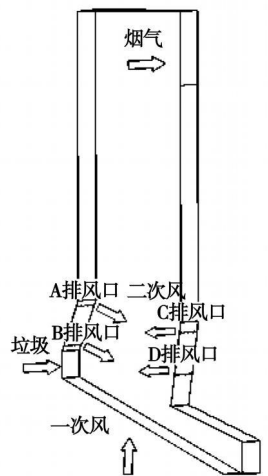


图 1 焚烧炉燃烧炉膛结构

表 1 入炉生活垃圾的元素分析和工业分析

数 值		数 值	
C	30.19	水分	14.7
H	3.79	挥发分	50
N	1.01	固定炭	7.7
S	0.07	灰分	27.6
O	22.08	低位热值/kJ·kg <sup>-1</sup>	11 183

1.2 富氧燃烧系统

为了保证可燃物质能够燃烧完全, 焚烧炉的空气过量系数大都在 1.5~1.9 之间, 有的甚至还大于 2.0。然而即使是这样, 燃烧温度、热灼减率等仍不是很理想。这主要是因为, 在焚烧过程中只能通过增加风量来满足燃烧过程需要的氧量。而且热解燃烧区风量过大, 反而会降低燃烧温度, 增加底渣和飞灰含碳量; 另外, 排烟热损失也会大幅度增加, 降低锅炉效率。

表 2 一次风气体组分

工况	1 号风室	2 号风室	3 号风室	4 号风室	5 号风室
1	空气(300 K)				
2	空气	O <sub>2</sub> =29%(v)	O <sub>2</sub> =31%(v)	空气	

表 3 二次风气体组分

工况	前墙		后墙	
	A 排风口	B 排风口	C 排风口	D 排风口
A	空气(300 K)			
B	361.3 K, O <sub>2</sub> =15.2%(v),	484.5 K, O <sub>2</sub> =8.6%(v),		
	CO <sub>2</sub> =9.8%(v)	CO <sub>2</sub> =12.4%(v)		
	N <sub>2</sub> =75%(v)	N <sub>2</sub> =79%(v)		

为此, 德国 Coburg 生活垃圾发电厂对 2 号焚烧炉进行了富氧燃烧技术改造。改造后的 2 号焚烧炉配置了烟气循环系统。纯液氧采用槽车运送。空气和纯氧混合后从炉排下方的第 2、3 个风室送入燃烧炉膛。循环的烟气经干燥吸收塔、过滤器和引风机后由循环泵从二次风口送入燃烧炉膛, 其中大部分的循环烟气从后墙的 C、D 两排风口送入, 少部分烟气和空气混合后从前墙送入。空气气氛和富氧气氛下、二次风的气体组分浓度和温度如表 2 和表 3 所示, 其中工况 B 烟气循环比例为 0.25。

为了对床层表面的燃烧温度实施实时监控, 在焚烧炉膛顶部安装了红外照相机, 并配备了相应的图像处理系统和燃烧控制系统。控制过程如下: 红

外摄影仪获得火焰温度数据, 传输到电脑, 进行图像处理并对火焰温度进行评估, 启动燃烧控制程序, 调整一次风量、氧气浓度及烟气循环比例。控制系统如图 2 所示。

电厂进行了为期一周的试运行: 2 号焚烧炉采用富氧燃烧技术后, 锅炉过量空气系数由 1.91 降到 1.43, 排烟量减少了 39%, 锅炉热效率提高了 7%; 主蒸汽量波动值由原来的 5% 降到 3%。但由于燃烧温度提高, 较多的灰渣黏结成块。

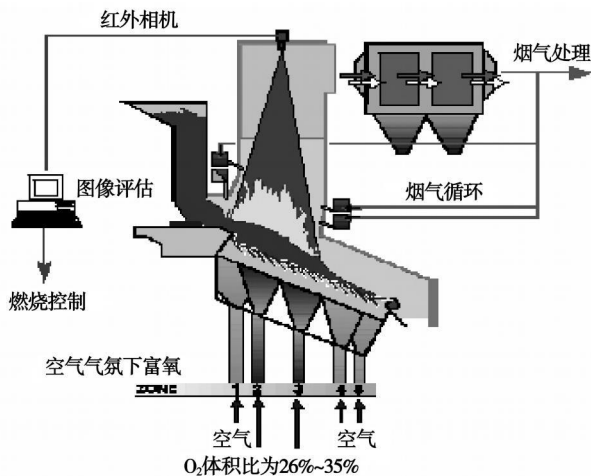


图 2 焚烧炉燃烧控制系统

2 数学模型及边界条件

垃圾在焚烧炉内的燃烧比较复杂, 为此将其在焚烧炉内的整个燃烧过程分成为两个子部分, 即垃圾在炉排上的燃烧和床层释放出的气体作为边界条件的上部炉膛空间的气相燃烧。两部分在不同的计算程序中进行, 炉排上的燃烧模拟为床层上方的气相燃烧提供烟气温度、速度和组分沿床层方向的分布, 而床层上方的气相燃烧模拟又为床层燃烧模拟提供其所需要的辐射强度。生活垃圾在炉排上的控制方程如下<sup>[6]</sup>:

连续性方程:

$$\frac{\partial \rho_{sb}}{\partial t} + \nabla \cdot (\rho_{sb}(V_s - V_B)) = S_s \quad (1)$$

能量方程:

$$\frac{\partial \rho_{sb} H_{is}}{\partial t} + \nabla \cdot (\rho_{sb}(V_s - V_B) H_{is}) = \nabla \cdot (\lambda_s \nabla T_s) + \nabla \cdot q_r Q_{sh} \quad (2)$$

气体组分方程:

$$\frac{\partial \rho_{sb} H_{is}}{\partial t} + \nabla \cdot (\rho_{sb}(V_s - V_B) Y_{is}) =$$

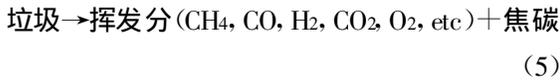
$$\nabla \cdot (D_s \nabla (\rho_{sb} Y_{is})) + S_{y_{is}} \quad (3)$$

动量方程:

$$\frac{\partial \rho_{sb} V_s}{\partial t} + \nabla \cdot (\rho_{sb} (V_s - V_B) V_s) = - \nabla \cdot \sigma -$$

$$\nabla \cdot \tau + \rho_{sb} g + A \quad (4)$$

一般地, 生活垃圾的热解反应可用以下的一步反应模型来描述:

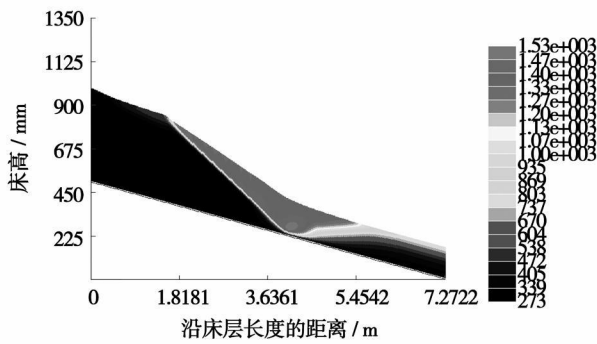


实际上, 燃烧气氛中氧气浓度的变化对垃圾的热解及燃烧是有影响的, 且该影响将反应到热解燃烧动力学参数上, 但当氧气浓度在一定的变化范围内 (< 30% (v)) 时, 该影响可暂不考虑<sup>[9-11]</sup>。

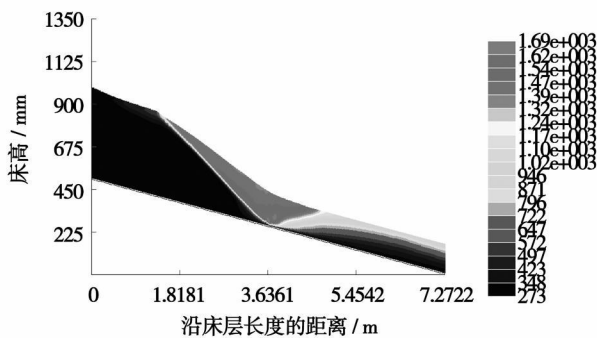
床层部分网格数量为 180×300, 控制方程采用 SIMPLE 算法求解。料层外的气相燃烧模拟采用有限速率/涡耗散反应模型, 粘性模型为 RNG k-ε 湍流模型, 辐射传热采用离散坐标辐射模型。床层外的燃烧炉膛空间共划分了 621 932 个网格。

### 3 计算结果与分析

#### 3.1 床层燃烧计算结果分析



(a) 工况1

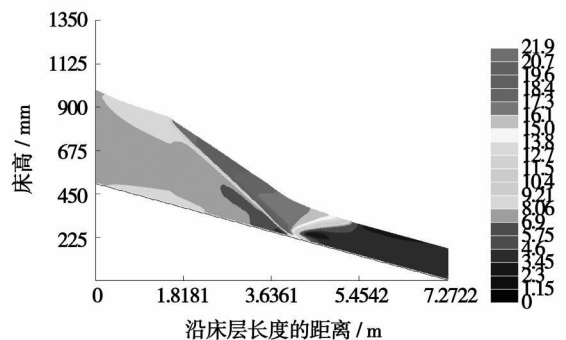


(b) 工况2

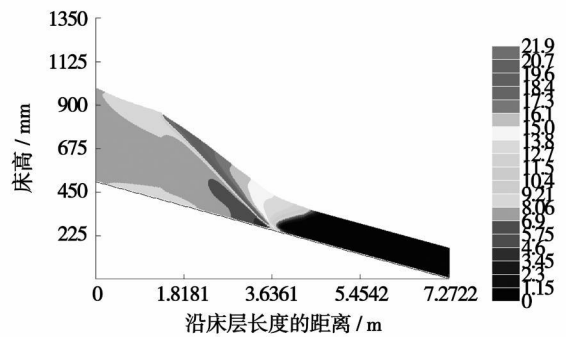
图 3 垃圾床层的温度分布(K)

新鲜的垃圾进入焚烧炉后受到炉拱、高温烟气

及火焰的辐射作用, 位于床层表面的垃圾团块温度首先升高, 水分开始蒸发。从图 3 可看到: 空气气氛下, 在床长约 1.6 m 处, 床层温度迅速升高到了 1 300 K, 即垃圾开始着火燃烧。随着燃烧的进行及炉排的运动作用, 燃烧反应区域向下扩展, 并且床层厚度逐渐降低, 但床层温度保持在一个比较平稳的范围内 (1 300~1 400 K), 说明此时垃圾正处于稳定的燃烧阶段。垃圾中水分不断减少, 也即水分蒸发吸收的热量减少, 床层温度有升高的趋势。在床长 4 m 处, 水分蒸发过程基本完成, 此时床层温度达到了最高值 1 530 K; 而富氧气氛下, 床层温度普遍较高, 且最高温度 (1 690 K) 出现在床长 3.5 m 处。之后, 床层温度都开始迅速降低。这主要是因为垃圾的含碳量低, 只有 7.7% (wt), 燃尽时间很短。实际上, 从图 4 焦炭质量分数分布图上可以看到, 大部分的焦炭已在床长 1.8~4.5 m 间燃烧。但到炉排尾部, 空气气氛下灰渣中仍有 4% (wt) 左右的焦炭没有完全燃烧, 而富氧气氛下则已基本上完全燃烧。



(a) 工况1

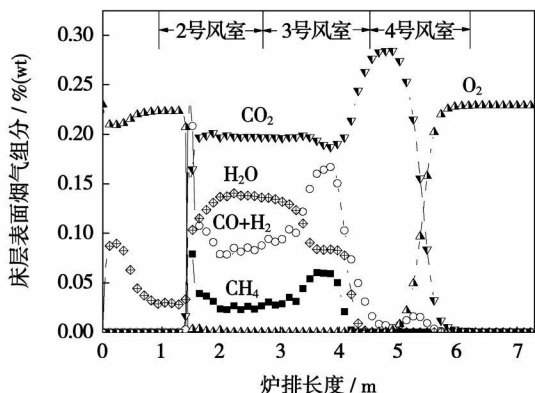


(b) 工况2

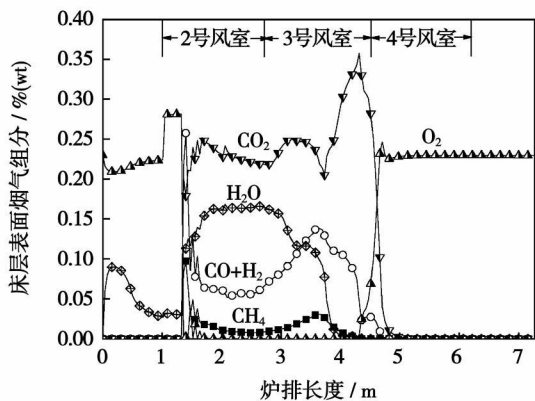
图 4 床层上的焦炭分布(%(wt))

图 5(b) 为富氧气氛下床层释放出的烟气组分沿床层长度的变化曲线。在第 1、2 风室的交接处, 氧气浓度出现了阶梯性的跳动, 即氧气浓度在 1 m 处由 22% (wt) 突然升高为 27% (wt)。但当垃圾着火燃烧时, 氧气浓度迅速降到只有 0.1% (wt) 左右, 且

在后续的稳定燃烧过程中，垃圾团块基本上都处于缺氧状态，这主要是因为大部分的可燃物质在此阶段燃烧，消耗了大量的氧气。在床长约 5 m 处，整个垃圾燃烧过程进入了最后的燃尽阶段，此时氧气浓度开始回升，并最终稳定在 20% (wt) 左右。另外，从图中还可以看出虽然提高了热解燃烧区的氧气浓度，但在燃烧过程中床层还是释放出了一定的可燃物质，如 CO, CH<sub>4</sub>, H<sub>2</sub> 等，但与空气气氛下相比，烟气可燃物含量是较少的。



(a) 工况1



(b) 工况2

图 5 富氧气氛下床层顶部烟气组分曲线

提高氧气浓度势必会加快燃烧反应速率。从图 6 两工况下床层上方烟气温度沿床层长度方向的变化曲线上可以看到，提高氧气浓度后，床层释放出的烟气温度突变点提前。一般可认为垃圾在此处着火燃烧。空气气氛下，烟气最高温度为 1 418 K，但基本上都在 1 350 K 处波动；实际测得在该工况下，燃烧区域的平均温度为 1 338 K<sup>[4]</sup>。而在富氧气氛下，烟气最高温度达到 1 663 K，燃烧区域的平均温度为 1 466 K，与实际测得平均温度 1 473 K 较吻合<sup>[4]</sup>。富氧燃烧气氛下，垃圾燃烧反应强度变大。在相同的炉排速度下，垃圾水分蒸发加快，使得燃烧过程提前进入了稳定燃烧和燃尽阶段。进入燃尽阶段后，

烟气温度迅速降低，但是炉排尾部上方的烟气温度比空气气氛下高近 100~150 K。这主要是因为富氧气氛下床层温度提高，而过量空气系数降低，炉排尾部送风量减少，加上较多的灰渣黏结成块，使得灰渣温度降低较为缓慢，烟温增加。

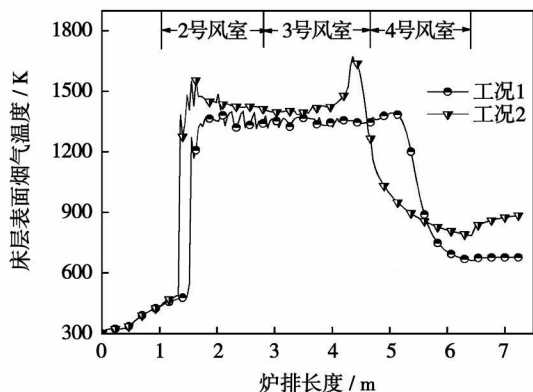


图 6 不同工况下床层上方烟气温度曲线

### 3.2 床层上方气相燃烧计算结果分析

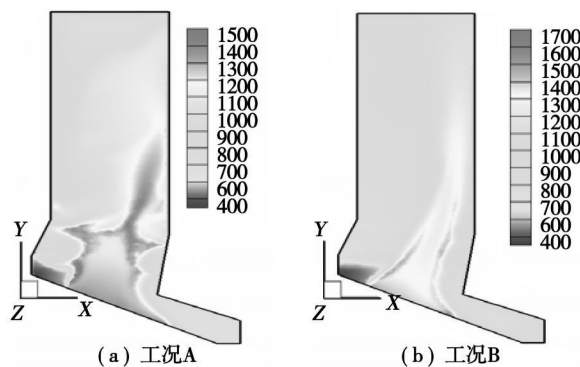


图 7 燃烧炉膛中截面的温度分布(K)

图 7 为燃烧炉膛中截面的温度分布。料层释放出的高温烟气中的可燃物质在床层上方的炉膛空间继续燃烧。空气气氛下，烟气中未燃尽的可燃物质较多，遇到高速的二次风后混合、燃烧，炉膛温度又开始升高，并且达到了床层表面烟气的温度水平，之后炉膛温度逐渐降低，到达燃烧炉膛出口处，面积平均温度为 1 078.6 K。富氧气氛下，炉膛温度并没有一个再次升高的过程，而是沿炉膛高度方向一直缓慢地降低。这可能是因为大部分的可燃物质在床层区域已燃烧，较少的气相可燃物在床层上方燃烧时放出的热量不足以抵消水冷壁吸收的热量，但到炉膛出口处面积平均温度仍有 1 123.5 K。

为了使可燃物能够燃烧完全并减少污染物的生成，炉膛出口的烟气氧量不应低于 6% (v)<sup>[5]</sup>。从图

8 两种气氛下燃烧炉膛中截面的氧气浓度分布可看到, 富氧气氛下, 炉膛出口氧气含量也达到了这一要求。实际运行中, 炉膛出口的烟气温度是通过烟气循环比例来控制, 而炉膛出口烟气氧量是通过改变一次风量及其氧含量来调整的。

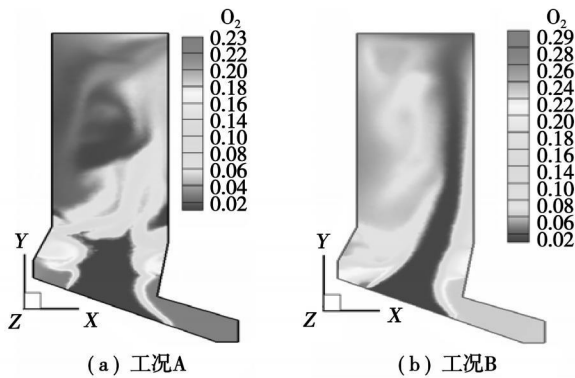


图 8 燃烧炉膛中截面的氧气浓度分布(%(v))

另外, 值得关注的是采用富氧燃烧/烟气循环技术后, 烟气流量减少, 炉内湍流度降低, 炉内烟气混合变差, 这对可燃物的完全燃烧是不利的。为改善气体在二次燃烧区域的燃烧混合, 应进行富氧烧嘴设计和炉型优化等相关工作, 以使焚烧炉能适应富氧燃烧技术。E. H. Chui 和 Ho Keun Kim 已对富氧燃烧器进行了理论设计研究<sup>[12-13]</sup>。

## 4 结 论

以德国 Coburg 生活垃圾发电厂 2 号焚烧炉为研究对象, 运用 CFD 技术探讨了富氧燃烧技术在生活垃圾焚烧处理方面的优势。虽然垃圾特性从水分、热值等都与国内的垃圾特性区别很大, 但在此模型的基础上, 可进一步研究国内高水分生活垃圾富氧燃烧的情况。通过数值计算结果和前人的试验数据可得到以下结论:

(1) 垃圾燃烧温度随着氧气含量的增加而升高。空气气氛下料层燃烧区域的平均温度为 1 350 K, 实际测量值为 1 338 K; 富氧气氛( $O_2/N_2=25:75$ )下料层燃烧区域的平均温度为 1 466 K, 测量值为 1 473 K。

(2) 提高一次风中的氧气含量, 垃圾着火位置向前移动。较高的燃烧温度加快了水分析出速率, 垃圾提前进入稳定燃烧和燃尽阶段; 灰渣中可燃物(焦炭)含量大幅度降低, 由 3.74 % (wt) 降为 0.1 % (wt)。

(3) 炉内气氛中氧气比例增加, 所需过量空气系数降低, 炉排尾部风量减少, 降低灰渣降温速率, 尾部烟气温度比空气气氛下高近 100~150 K。

(4) 氧气浓度提高, 烟气流量减少, 湍流度降低, 炉内烟气混合减弱, 应采取相应措施, 如设计新的燃烧器或对炉膛结构配风进行一定的优化以使焚烧炉适应富氧燃烧, 最大限度地减少污染物的生成和排放。

## 参考文献:

- [1] CHARLES E, BAUKAL JR. Oxygen-enhanced combustion[M]. Washington: CRC Press, 1999.
- [2] GOHLKE O, BUSCH M. Reduction of combustion by-products in WTE plants  $O_2$  enrichment of underfire air in the martin syncom process[J]. Chemosphere, 2001, 42: 545-550.
- [3] MELO G F, IACAVAL P T, GARVAIHO J A. A case study of air enrichment in rotary kiln incineration[J]. International Communications in Heat and Mass Transfer, 1998, 25(5): 681-692.
- [4] MULLER ROOSEN, RINGEL M H. Studies on the high-temperature incineration of polymer-containing special waste with oxygen enrichment[J]. Chem Eng Technol, 2002, 23(12): 1069-1072.
- [5] GIUSEPPE LIUZZO, NICOLA VERDONE, MARCO BRAVI. The benefits of flue gas recirculation in waste incineration[J]. Waste Management, 2006, 27: 106-117.
- [6] YANG Y B, LIM C N, GOODFELLOW J, et al. A diffusion model for particle mixing in a packed bed of burning solids[J]. Fuel, 2005, 84: 213-225.
- [7] YANG Y B, GOH Y R, ZAKARIA R, et al. Mathematical modelling of MSW incineration on a travelling bed[J]. Waste Management, 2002, 22(4): 369-380.
- [8] YANG Y B, SHARIFI V N, SWITHENBANK J. Converting moving-grate incineration from combustion to gasification-numerical simulation of the burning characteristics[J]. Waste Management, 2007, 27(5): 645-655.
- [9] FANG M X, SHEN D K, LI Y X, et al. Kinetic study on pyrolysis and combustion of wood under different oxygen concentrations by using TG-FTIR analysis[J]. Journal of Analytical and Applied Pyrolysis, 2006, 77(1): 22-27.
- [10] LIU GUO HUI, MA XIAO QIAN, YU ZHAOSHENG. Experimental and kinetic modeling of oxygen-enriched air combustion of municipal solid waste[J]. Waste Management, 2009, 29: 792-796.
- [11] SENNECA O, CHIRONE R, SALATINO P. Oxidative pyrolysis of solid fuels[J]. Journal of Analytical and Applied Pyrolysis, 2004, 71(2): 959-970.
- [12] CHUI E H, MAJESKI A J. Numerical investigation of oxy-coal combustion to evaluate burner and combustor design concepts[J]. Energy, 2004, 29: 1285-1296.
- [13] HO KEUN KIM, YONGMO KIM. NO reduction in 0.03~0.2 MW oxy-fuel combustor using flue gas recirculation technology[J]. Proceedings of the Combustion Institute, 2007, 31: 3377-3384.

(编辑 单丽华)

to be solved for using low-heat-value fuels. **Key words:** biomass, low heat value, miniature gas turbine

合成气-甲醇掺烧火焰研究= **Investigation of Mixing-dilution Combustion Flames of Syngas-methanol**[刊, 汉]/ ZHANG Wen-xing, MU Ke-jin, WANG Yue, et al (Key Laboratory on Advanced Energy and Power, Institute of Engineering Thermophysics, Chinese Academy of Sciences, Beijing, China, Post Code: 100190)// Journal of Engineering for Thermal Energy & Power. — 2009, 24 (2). — 236 ~ 241

An experimental study and numerical analysis was performed of the mixing-dilution combustion flames of syngas-methanol. During the experiment, the flame morphology was observed, and the flame temperature as well as the concentration of  $\text{NO}_x$  pollutants in the flue gas were measured. The test results show that under the condition of an equal power output, the shape of the mixing-dilution combustion flame of the syngas-methanol seems slightly slender as compared with that of a syngas flame, the temperature in the high-temperature zone is a bit low and the  $\text{NO}_x$  emissions from the flue gas are comparatively small. A numerical calculation and analysis shows that the mixing-dilution combustion flame in question becomes longer, because the methanol in the flame has not been burnt out in time, and the drop of flame temperature comes about from a relatively low temperature of the methanol flame. The decrease of  $\text{NO}_x$  emissions from the flue gas results from the addition of methanol to the flame, which is conducive to suppressing the formation of NO of both the thermal and intermediate type. **Key words:** syngas, methanol, mixing-dilution combustion,  $\text{NO}_x$

湿法脱硫的传质与化学平衡模型研究= **Study of a Model Featuring Mass Transfer and Chemical Equilibrium for Wet Method-based Desulfuration**[刊, 汉]/ ZHANG Xiao-dong, WANG Xiu-yan (College of Energy Source and Power Engineering, North China Electric Power University, Beijing, China, Post Code: 102206), ZHENG Yong-gang (College of Resources and Environmental Science, Chongqing University, Chongqing, China, Post Code: 400044)// Journal of Engineering for Thermal Energy & Power. — 2009, 24(2). — 242 ~ 246

The technology of limestone-gypsum wet-method desulfuration by using a spray absorption tower is nowadays most widely used in coal-fired power plants. Inside the tower, the sprinkling liquid droplets will fall in an inverse direction against the rising flue gas flow to absorb  $\text{SO}_2$  in the flue gas. Based on a steady-state assumption, the authors analyzed the equilibrium relationship between the chemical reaction process in the droplets and liquid-phase constituents, and also presented a model featuring the dissolution velocity of solid  $\text{CaCO}_3$ . By employing a total mass transfer coefficient, set up was a mass transfer rate model for droplet absorption-phase constituents. Through an analysis of the material quantity equilibrium of various components between the gas and liquid phases, established was an equilibrium equation for the controlled volume in the absorption zone. The model in question can provide guidance for relevant engineering applications, and can also be used for the emulation calculation of absorption towers and flow-field numerical simulation calculations. **Key words:** absorption tower, flue gas desulfuration, controlled volume, mass transfer rate

利用 CFD 技术对城市生活垃圾富氧燃烧特性分析= **Research on the Characteristics of MSW (Municipal Solid Waste) Oxygen-enriched Combustion Based on Computational Fluid Dynamics**[刊, 汉]/ LIU Guo-hui, MA Xiao-qian, YU Zhao-sheng (College of Electric Power, South China University of Technology, Guangzhou, Post Code: 510640)// Journal of Engineering for Thermal Energy & Power. — 2009, 24(2). — 247 ~ 251

The oxygen-enriched combustion technology enjoys conspicuous benefits of energy-saving and environment protection, and represents an effective measure for achieving a steady combustion of low-heat-value wastes and reducing pollutant emissions. By employing CFD (Computational Fluid Dynamics) technology, studied were the characteristics of MSW (Municipal Solid Waste) combustion in the oxygen-enriched atmosphere of a mechanical stoker. The authors have presented the curves showing the flue gas temperature and constituent concentration over and above the waste-burning bed layer as well

as the bed layer coke distribution under the following two operating conditions, i. e.  $O_2/N_2=21:79$  and  $O_2/N_2=25:75$ . The simulation results show that when the oxygen concentration of the primary air is increased from 21% to 25% (by volume), the average temperature of the combustion zone on the surface of MSW bed layer will rise from 1 350 K to 1 466 K, namely, an increment of 116 K. The combustible (coke) content of ash slag will decline from 3.9% to 0.1% (by weight). With an increase of oxygen concentration, the ignition location of the MSW will shift forward with the MSW entering a steady combustion stage ahead of schedule. The simulation results are in good agreement with the test ones measured by predecessors. **Key words:** municipal solid waste (MSW), incineration, oxygen enrichment, numerical simulation, Martin reciprocating grate

10 ~ 100 mm 长度的棉秆在流化床中的燃烧特性 = **Combustion Characteristics of Cotton Stalks of 10 to 100 mm in Length Burnt in a Fluidized Bed** [刊, 汉] / SUN Zhi-ao, JIN Bao-sheng, ZHANG Ming-yao (College of Energy Source and Environment, Southeast University, Nanjing, China, Post Code: 210096) // Journal of Engineering for Thermal Energy & Power. — 2009, 24(2). — 252 ~ 256

Described were the physicochemical characteristics of cotton stalks of 10 to 100 mm in length and their ash. With high alumina bauxite serving as bed material, and on a fluidized bed test rig having a thermal power output of 0.2 MW, the combustion characteristics of pure cotton stalks in question were studied under different operating conditions. It has been found that when the fluidization number  $N$  is greater than 3, the temperature in a dense-phase zone ranging from 850 to 880 °C, and a stable combustion can be maintained, indicating that the cotton stalks and the bed material can be mixed relatively well. During the test, the concentration of main pollutant emissions was measured. After a continuous operation of 38 hours, the bed material has basically kept its original shape and appearance unchanged, and no agglomeration phenomena emerged. The tests show that the pure cotton stalks can adapt themselves to combustion in fluidized beds, and this is of major significance for guiding commercial applications on a large scale. **Key words:** long cotton stalk, bed material, fluidized bed, combustion characteristics

混流式水轮机导叶叶道内湍流场的大涡模拟 = **Large Eddy Simulation of the Turbulent Flow Field in Guide Vane Flow Passages of a Mixed-flow Type Water Turbine** [刊, 汉] / WANG Wen-quan, ZHANG Li-xiang, YAN Yan, et al (Department of Engineering Mechanics, Kunming University of Science and Technology, Kunming, China, Post Code: 650093) // Journal of Engineering for Thermal Energy & Power. — 2009, 24(2). — 257 ~ 260

By using the  $N-S$  control equation of a nonsteady incompressible fluid and the dynamic sub-grid turbulence model of a large eddy simulation, and based on mixed grid techniques, the authors have employed SIMPLC algorithm to seek separate solutions to velocity and pressure variables. As a result, obtained were the distribution of velocity field, pressure field and vorticity field in the whole flow passages of the movable guide vanes of an A55x type test-model water turbine. The calculation results show that the eddy belt formed by the stream encircling the movable guide vanes further develops downstream, leading to a nonuniform velocity and pressure distribution at the inlet of the rotating wheel and exercising a direct influence on the flow state inside the wheel. In the meanwhile, studied were the dynamic characteristics of the nonuniform flow field after the guide vanes. It has been found that the closer to the downstream, the smaller the time-averaged pressure and speed nonuniformity. However, the values of transient nonuniformity at various cross sections have a relatively big difference. It is proposed that to identify the cross section, which always has the minimum time-averaged speed nonuniformity after the blades, should become an important design effort and index for the hydraulic design of future water turbines. **Key words:** energy source and power engineering, flow field dynamic characteristics, guide vane flow passage, large eddy simulation, dynamic sub-grid model